


## PAPER

[View Article Online](#)  
[View Journal](#) | [View Issue](#)Cite this: *Nanoscale Adv.*, 2023, 5, 1691

# The potential role of serum extracellular vesicle derived small RNAs in AML research as non-invasive biomarker†

Lin Li, <sup>‡\*a</sup> Veronika Mussack,<sup>‡b</sup> André Görgens,<sup>cd</sup> Elena Pepeldjiyska,<sup>a</sup> Anne Sophie Hartz,<sup>a</sup> Hazal Aslan,<sup>a</sup> Elias Rackl,<sup>a</sup> Andreas Rank,<sup>e</sup> Jörg Schmohl,<sup>f</sup> Samir El Andaloussi,<sup>c</sup> Michael W. Pfaffl<sup>§b</sup> and Helga Schmetzer<sup>§\*a</sup>

**Background:** Extracellular vesicles (EV) are cell-derived vesicles released by all cells in health and disease. Accordingly, EVs are also released by cells in acute myeloid leukemia (AML), a hematologic malignancy characterized by uncontrolled growth of immature myeloid cells, and these EVs likely carry markers and molecular cargo reflecting the malignant transformation occurring in diseased cells. Monitoring antileukemic or proleukemic processes during disease development and treatment is essential. Therefore, EVs and EV-derived microRNA (miRNA) from AML samples were explored as biomarkers to distinguish disease-related patterns *ex vivo* or *in vivo*. **Methodology:** EVs were purified from serum of healthy (H) volunteers and AML patients by immunoaffinity. EV surface protein profiles were analyzed by multiplex bead-based flow cytometry (MBFCM) and total RNA was isolated from EVs prior to miRNA profiling via small RNA sequencing. **Results:** MBFCM revealed different surface protein patterns in H *versus* AML EVs. miRNA analysis showed individual as well as highly dysregulated patterns in H and AML samples. **Conclusions:** In this study, we provide a proof-of-concept for the discriminative potential of EV derived miRNA profiles as biomarkers in H *versus* AML samples.

Received 30th December 2022  
Accepted 13th February 2023

DOI: 10.1039/d2na00959e

[rsc.li/nanoscale-advances](http://rsc.li/nanoscale-advances)

## Introduction

### Acute myeloid leukemia (AML)

AML is characterized by an uncontrolled and excessive proliferation and an impaired differentiation of myeloid progenitor cells, leading to an expansion of leukemic cells (blasts) in the

bone marrow (BM), peripheral blood (PB) and other tissues, going along with a replacement of the physiological hematopoiesis, leading to anemia, bleeding and infections.<sup>1,2</sup> In order to fight AML, several (immune) therapeutic cellular, antibody based or chemotherapeutic strategies have been developed (*e.g.* checkpoint blockades, chimeric antigen receptor (CAR)-T cell therapies and vaccinations or immune modulating hypomethylating agents).<sup>3,4</sup> Currently, the major challenge is still in the development of effective (immune) therapies in AML to overcome many immunosuppressive mechanisms.<sup>4</sup>

### Extracellular vesicles (EVs)

The term 'EVs' comprises a broad variety of extracellular vesicle types with overlapping chemical and biophysical properties, including exosomes (which originate from the endocytic system) and microvesicles or ectosomes (formed by budding from the plasma membrane).<sup>5</sup> EVs carry and deliver essential molecular information for cell physiology and metabolism. Overall, their composition, concentration and biodistribution as well as the functional role in intercellular signaling can impact the general health status, but EVs also can play a role in pathological events, including malignant transformations of cells.<sup>6</sup> In hematological malignancies, tumor- or immune cell-derived EVs might reprogram the bone marrow environment, suppress or activate anti-leukemic immune response, modulate

<sup>a</sup>Immune-Modulation, Medical Department III, University Hospital of Munich, Marchioninistraße 15, 81377 Munich, Germany. E-mail: Lin.Li0814@outlook.com; elena.pepeldjiyska@gmail.com; as.hartz@t-online.de; hazlaslan@gmail.com; elias.rackl@hotmail.de; Helga.Schmetzer@med.uni-muenchen.de; Fax: +49 89 4400 76137; Tel: +49 89 4400 73137

<sup>b</sup>Department of Animal Physiology and Immunology, TUM School of Life Sciences Weihenstephan, Technical University of Munich, Freising, Germany. E-mail: veronika.mussack@mytum.de; michael.pfaffl@tum.de

<sup>c</sup>Department of Laboratory Medicine, Division of Biomolecular and Cellular Medicine, Karolinska Institutet, Stockholm, Sweden. E-mail: andre.gorgens@ki.se; Samir.El-Andaloussi@ki.se

<sup>d</sup>Institute for Transfusion Medicine, University Hospital Essen, University of Duisburg-Essen, Essen, Germany

<sup>e</sup>Department of Hematology and Oncology, University Hospital of Augsburg, Augsburg, Germany. E-mail: andreas.rank@uk-augsburg.de

<sup>f</sup>Department of Hematology and Oncology, Hospital of Stuttgart, Stuttgart, Germany. E-mail: joerg.schmohl@diak-stuttgart.de

† Electronic supplementary information (ESI) available. See DOI: <https://doi.org/10.1039/d2na00959e>

‡ Lin Li and Veronika Mussack contributed equally.

§ Michael W. Pfaffl and Helga Schmetzer contributed equally.

drug resistance, and could therefore interfere with immunotherapies.<sup>7,8</sup> Composition of EVs collected from patients' serum might correlate with disease stage, drug- and/or immunological resistance, or response to (immune) therapies.<sup>9</sup>

A comprehensive EV purification and characterization to provide high reproducibility and comparability of data is necessary.<sup>10</sup> According to MISEV guidelines,<sup>5</sup> EVs can be enriched by various methods,<sup>11</sup> e.g. ultra-centrifugation, precipitation, size exclusion chromatography, ultrafiltration, immunoaffinity-based binding strategies. Obtained EVs can be characterized by multiple methods to assess purity and specificity.<sup>12</sup> Vesicular surface marker expressions (e.g. CD9, CD63, CD81) can be studied using flow cytometry, size and concentration measurements by fluorescence nanoparticle tracking analysis (fNTA).<sup>13,14</sup> EV morphology can be investigated by Transmission Electron Microscopy (TEM).<sup>15</sup> Western blotting is used to assess the presence of EV specific and non-specific (surface) protein markers. Detailed phenotyping of EV subsets co-expressing specific pairs of protein surface markers can be achieved for instance through high resolution single vesicle imaging flow cytometry (IFCM)<sup>16</sup> or by multiplex bead-based flow cytometry (MBFCM). The MBFCM assay includes 39 hard-dyed capture bead populations, each of them coated with different monoclonal antibodies against 37 potential EV surface antigens or two internal isotype negative controls.<sup>13</sup>

### Characteristics and potential of small RNAs

MicroRNAs (miRNA) are evolutionarily conserved small non-coding RNAs (20–24 nucleotides) and have important physiological effects through their post-transcriptional gene regulation mainly by repression of target messenger (m)RNA.<sup>17,18</sup> It has been discovered that miRNAs are released into various body fluids in complexes with lipoproteins, soluble proteins or encapsulated in EVs.<sup>7</sup> EV-associated miRNAs as well as other molecular cargo can be shuttled to recipient cells *via* transfer through the blood circulation, which plays an important role in long distance cell-to-cell communication.<sup>19</sup>

Beyond dysregulated miRNA expression profiles, it is now well accepted that selected cellular/extracellular miRNAs can function as either tumor activating (oncomiRs) or tumor suppressing miRNAs in many subtypes of tumor processes, including tumor proliferation, survival, differentiation, self-renewal, epigenetic regulation, going along *in vivo* with chemotherapy resistance and disease progression.<sup>7,17</sup> These observations indicate that the circulating miRNA profiles may reflect physiological and pathological processes occurring in different cells and tissues, and might qualify as valuable blood-based biomarkers for various diseases.<sup>7</sup>

Biomarker research has already shown, that EV marker profiles and their miRNA cargo might contribute to monitor the disease as well as the (antileukemic) immune status and to select risk-adapted therapies.<sup>20</sup> These findings might be used as a powerful tool to detect both novel and known (EV-derived) miRNAs that could qualify as biomarkers.

The aim of this study was to (1) prepare and characterize EVs from serum samples of healthy donors and AML patients; (2)

evaluate the use of MBFCM for comparing the overall EV surface protein composition on EVs in minimally processed samples from healthy donors *versus* AML patients; and (3) assess EV-associated miRNA profiles that could be applied as potential biomarkers comparing healthy donors' with AML patients' serum.

## Material and methods

### Sample preparation

Blood sample collection was conducted after obtaining written informed consent of the blood donor and in accordance with the World Medical Association Declaration of Helsinki and the ethic committee of the Ludwig-Maximilians-University-Hospital Munich (vote no. 33905). Serum samples were collected with 4.5 ml serum tubes (S-Monovette) and provided by the University Hospitals of Augsburg, Stuttgart and Munich. Around 3 ml of serum were isolated from each healthy or AML donors' sample. Cells and larger particles were sedimented from serum after centrifugation (2000×g, 10 min, room temperature). The resulting supernatant (containing EVs) was aliquoted in 0.5 ml tubes and stored at –80 °C until further processing.

Serum samples were obtained from healthy (H) volunteers ( $n = 5$ ) with a mean age of 28.6 (range 24–31 years) and from AML patients ( $n = 5$ ) with a mean age of 77 years (range 61–98 years). AML patients were classified by the French–American–British (FAB)-classification (M1–M7), the aetiology (primary or secondary AML), the stage of disease (first diagnosis, relapse) and the frequencies of blasts and blast phenotype are given in Table 1.

Flow cytometric analyses were carried out to evaluate and quantify frequencies and phenotypes of blasts, T-, B- and monocyte subsets in the WB-fractions. Panels with various monoclonal antibodies (moAbs) labeled with fluorescein isothiocyanate (FITC), phycoerythrin (PE), tandem Cy7-PE conjugation (Cy7-PE), or allophycocyanin (APC) were used. Erythrocytes in blood samples were lysed using Lysing-Buffer (BD, Heidelberg, Germany). Cells dissolved in PBS (Biochrom, Berlin, Germany) and 10% fetal calf-serum (FCS, Biochrome, Berlin, Germany) were performed by a 15 min incubation in the dark at room temperature. Afterwards, the cells were washed, centrifuged, resuspended in 100–200  $\mu$ L PBS and measured using fluorescence-activated cell sorting flow-cytometer (FACSCalibur™) and Cell-Quest-data-acquisition and analysis software (Becton Dickson, Heidelberg, Germany). Isotype controls were conducted according to manufacturer's instructions.<sup>21</sup> The cellular composition of AML patients presented an average of 44.4% (immune cytologically detected, IC) blasts (range 30–72), 14.74% CD3+ cells (range 7.14–27.68), 3.88% CD19+ cells (range 1.32–6.98), 27.37% CD56+ cells (range 7.18–64.58), and 10.53% CD14+ (range 3.81–28.18). H-controls presented with 10.51% CD3+ cells (range 1.27–20.69), 1.33% CD19+ cells (range 0.28–2.38), 6.38% CD56+ cells (range 1.41–11.95), and 3.15% CD14+ (range 0.47–5.43). In case of aberrant CD56 or CD14 expression on blasts, these values were excluded from NK/monocytes quantification. An overview is given in Table 2.





Table 1 Patients' and healthy individuals' characteristics<sup>a</sup>

	Pat. no.	Age/sex	Dgn. subtypes	Stage	IC blasts (%)	Blast phenotype (CID)	Risk stratification <sup>b</sup>	WBC [G/l]	Hb [g dL <sup>-1</sup> ]	PLT [G L <sup>-1</sup> ]	Response to (induction)-chemotherapy
AML	1567	98/F	pAML	Dgn	16	34, 117, 56, 14, 15, 65	Adverse	7.96	8.3	12	NCR
	1597	84/F	sAML	Dgn	72	117, 34, 56, 65, 15, 33, 13	Intermediate	88.6	11.3	41	NCR
	1609	72/M	sAML	Dgn	59	117, 34, 56, 65, 33	Favourable	10.04	9.5	114	CR
	1594	70/F	pAML/M4	Pers.	30	34, 117, 13, 33, 65	Favourable	1.32	6.8	125	NCR
	1598	61/F	sAML	Rel.	45	117, 33, 13	Adverse	19.6	8.3	15	NCR
H	1579	31/M	nd	nd	nd	nd	nd	nd	nd	nd	nd
	1580	24/F	nd	nd	nd	nd	nd	nd	nd	nd	nd
	1583	29/M	nd	nd	nd	nd	nd	nd	nd	nd	nd
	1585	30/M	nd	nd	nd	nd	nd	nd	nd	nd	nd
	1586	29/M	nd	nd	nd	nd	nd	nd	nd	nd	nd

<sup>a</sup> AML acute myeloid leukemia; H healthy; Pat. no. patient's number; F female; M male; p primary AML; s secondary AML; CD cluster of differentiation; dgn first diagnosis; Hb hemoglobin; IC blast immune cytologically detected blasts; bold markers used to quantify blasts; nd no complete remission; NCR no complete remission; pers. persisting disease; PLT platelets; WBC white blood cells; nd, no data. <sup>b</sup> AML patients were classified based on the National Comprehensive Cancer Network (NCCN) guidelines as "favorable", "intermediate", or "adverse risk".

Table 2 Cellular composition of H and AML samples

	Pat. no.	CD14+ expressing cells (%)	CD19+ expressing cells (%)	CD3+ expressing cells (%)	CD56+ expressing cells (%)
AML	P1567	28.18 <sup>a</sup>	2.74	7.14	44.9 <sup>a</sup>
	P1594	9.42	2.56	16.91	8.18
	P1597	6.02	1.32	9.29	64.58 <sup>a</sup>
	P1598	3.81	5.81	12.68	7.18
	P1609	5.22	6.98	27.68	12 <sup>a</sup>
H	1579	2.94	2.38	12.73	3.21
	1580	5.43	1.14	8.71	11.95
	1583	3.12	0.72	9.13	4.38
	1585	0.47	0.28	1.27	1.41
	1586	3.8	2.12	20.69	10.94

<sup>a</sup> (Aberrant) expression of these markers on leukemic cells; AML acute myeloid leukemia; H healthy donors; Pat. no. patient's number.

### Extracellular vesicle preparation

1.27 ( $\pm 0.09$ ) ml were used as input volume for EV isolation using Exosome Isolation Kit, pan, human (Miltenyi Biotec) according to the manufacturer's instructions which includes a further centrifugation step at  $10\,000\times g$  for 45 min at room temperature.

### EV characterization

As recommended by MISEV2018 guidelines,<sup>5</sup> purified EVs were characterized by TEM and fNTA as described before.<sup>22</sup>

### Multiplex bead-based flow cytometry (MBFCM)

Serum samples (each tube 0.5 ml) were thawed and subjected to MBFCM (MACSplex Exosome Kit, human, Miltenyi Biotec).<sup>13,22</sup> EV-containing serum samples were centrifugated at  $2500\times g$  for 15 minutes before supernatants were processed. 30  $\mu$ L of each sample was diluted with 30  $\mu$ L MACSplex buffer (MPB) and loaded onto wells of a pre-wet and drained MACSplex 96-well 0.22  $\mu$ m filter plate. Next, 8  $\mu$ L of MACSplex Exosome Capture Beads (containing 39 different antibody-coated bead subsets) were added to each well as described elsewhere.<sup>22</sup>

Surface proteins included in the MBFCM assay comprise the tetraspanins CD9, CD63, and CD81, and other surface proteins such as various leukocyte, T cell (CD4, CD8), B cell (CD19, CD20, CD24), monocyte (CD14), thrombocyte (CD41b, CD42a, CD62P, CD69), integrin (CD11c (integrin  $\alpha$ X or CR4), CD29 (integrin  $\beta$ 1), CD41b (integrin  $\alpha$ II $\beta$ ), CD49e (integrin  $\alpha$ 5)), endothelial (CD31, CD105, CD146 (Mel-CAM)), or MHC-associated (HLA-ABC (MHC-I), HLA-DRDPDQ (MHC-II)) antigens.

In this study, we removed values for capture beads coated with hIgG (REA) antibodies for the samples AML P1598 and H P1580 due to high background signals for internal hIgG (REA) isotype control beads. Background-subtracted median APC fluorescence values  $<1$  were considered negative ( $\sim 2$  fold average mIgG/REA control bead SD).

### Extracellular RNA isolation

Total RNA of a complete EV eluate was isolated using the miRNeasy Mini Kit (Qiagen, Germany) according to the manufacturer's protocol. The obtained RNA eluate was applied twice to the membrane to obtain higher RNA yields. The resulting eluate of 30  $\mu$ L was completely vacuum-evaporated and resolved in a total volume of 12  $\mu$ L nuclease-free water.

Isolated RNA was quality controlled and quantified by capillary gel electrophoresis using the RNA 6000 Pico Kit (Agilent Technologies, Germany) and the Bioanalyzer 2100 (Agilent Technologies). Total RNA was stored at  $-80^\circ\text{C}$  until small RNA-Seq library preparation.

### Small RNA library preparation and sequencing reaction

Equal amounts of RNA of the biological replicates were pooled, and 6.0 ng total RNA were used as starting material for library preparation using the NEBNext Multiplex Small RNA Library Prep Set for Illumina (New England Biolabs, USA) in accordance with the manufacturer's instructions. After a pre-amplification,

PCR products were purified by applying the Monarch PCR Cleanup Kit (New England Biolabs). Then, cDNA libraries were evaluated *via* capillary gel electrophoresis using the DNA 1000 Kit and the Bioanalyzer 2100 (Agilent Technologies) according to the manual. A miRNA-specific length of 130–150 base pairs of barcoded cDNA libraries was selected by applying and fractionating 5 ng of pooled cDNA on a 4% agarose gel (MetaPhor, USA). Clean-up of cut gel slices at the appropriate size range was performed using the Monarch Gel Extraction Kit (New England Biolabs) and correct size and molarity were analyzed *via* capillary gel electrophoresis using the Bioanalyzer DNA High Sensitivity Kit (Agilent Technologies). Finally, 50 cycles of single-end sequencing-by-synthesis reactions were conducted on the HiSeq 2500 instrument (Illumina, USA) with the HiSeq Rapid SBS Kit v2 (Illumina, USA).

### Small RNA-Seq data analysis

The Quality Phred Score generated by the FastQC software (Babraham Bioinformatics, UK, Version 0.11.9) was used to explore successful sequencing.<sup>23</sup> Next, 3' adapter sequences were trimmed from raw sequencing reads using Btrim.<sup>24</sup> In case no adapter could be detected or reads appeared with less than 16 nucleotides, the respective reads were discarded. Residual reads were aligned to sequences provided by RNA-central v12.<sup>25</sup> Reads that mapped to ribosomal RNA (rRNA), small nuclear RNA (snRNA), small nucleolar RNA (snoRNA), or transfer RNA (tRNA) were not considered in further processing. Remaining reads were then mapped to human precursor miRNA sequences while allowing for one mismatch (miRBase, release 22.1 and Bowtie).<sup>26,27</sup> Reads that still remained unmapped were named as such and not processed further. Read count tables were created by summing up all hits per specific sequence.

### Statistical analysis

Data is presented as mean  $\pm$  SD unless otherwise stated. For comparison of two groups a paired *t*-test was applied. Differences were considered as 'not significant' with (adjusted) *p*-values  $> 0.1$ , as 'borderline significant' (#) with (adjusted) *p*-values between 0.05 and 0.1, as 'significant' (\*) with (adjusted) *p*-values between 0.01 and 0.05, as 'highly significant' (\*\*) with (adjusted) *p*-values between 0.001 and 0.01, as 'very highly significant' (\*\*\*) with (adjusted) *p*-values between 0.0001 and 0.001 and as 'extremely significant' (\*\*\*\*) with (adjusted) *p*-values  $< 0.0001$ . Statistical analyses and creation of diagrams were performed using Microsoft Excel 2016, GraphPad Prism version 8.4.0 and R programming language, version 4.1.0.

Processed by the Bioconductor package DESeq2 (version 1.20.0) and pheatmap (version 1.0.12), only miRNAs with more than 20 DESeq2-normalized reads were treated as valid. Exploratory data analysis was visualized by Venn diagram, hierarchical clustering and heatmap analysis based on Euclidean distances. Differential gene expression was assessed by calculating miRNA-specific log<sub>2</sub> fold changes (FC).





## Results

We aimed to establish a proof-of-concept workflow to evaluate EV-associated miRNA profiles as potential diagnostic, prognostic or predictive markers to predict immune reaction, clinical subvision or response to treatment in AML patients compared to healthy volunteers.

Typical cup-shaped appearance of serum EVs were identified by TEM and EV concentrations and size distribution profiles of purified serum EV samples from H and AML patients by fNTA, as shown before.<sup>22</sup> In this manuscript, we focused on the quantitative and qualitative assessment of EV surface characteristics *via* MBFCM and especially the characterization of the EV-derived miRNA cargo by RNA-Seq to evaluate their potential as biomarkers in AML samples compared to healthy volunteers.

### EV surface protein profiles of H and AML samples by MBFCM

The MBFCM assay is based on the co-detection of two EV surface markers: one marker (based on the fluorescence-labelled detection antibody), aims to detect all tetraspanin-positive EVs bound to the respective capture bead, which is a mixture of pan anti-tetraspanin (CD9, CD63, CD81) antibodies. Another marker (based on specificity of one of 37 capture beads) is coated with specific capture antibodies.<sup>28</sup> The principle of MBFCM make sure that only EVs are directly captured, not free proteins, without further purification, specific detection of EVs are identified.<sup>13</sup>

In this study we included serum from 5 H and 5 AML samples (Table 1) and analyzed the EV surface protein profiles by MBFCM. An overview presentation of results showed that EV markers CD81, CD63, CD9 and in addition lineage markers

CD8, CD41b, CD42a, CD62P, HLA-DRDPDQ and SSEA-4 markers were both highly expressed on H and AML derived EVs (Fig. 1). Comparing individual EV markers in AML and H samples, we found differences for some markers (Fig. 2).

### Characterization of extracellular vesicle associated RNA by RNA-Seq

To systematically characterize the miRNA profiles associated with serum-derived EVs, we performed small RNA-Seq analysis in 5 AML and 5 H sample pools. First, total RNA was extracted from purified EVs. Quality control using capillary gel electrophoresis revealed low average RIN values of 1.6 ( $\pm 0.5$ ) for RNA samples obtained from H derived EVs and 1.7 ( $\pm 1.6$ ) for RNA samples obtained from AML derived EVs. This is a typical range for EV-associated RNAs, as EVs are considered to have minimum amounts of ribosomal 18S and 28S rRNA amounts, mostly bound to the EV surface. Further, total EV-associated RNA yields of 2.1 ( $\pm 0.8$ ) ng (H) and 2.5 ( $\pm 1.1$ ) ng (AML) were quantified, respectively.

Furthermore, small RNA-Seq was conducted to analyze the miRNA cargo of EVs. In total, in average  $8.7 \times 10^6$  reads were detected in serum-derived EVs from H samples and  $14.2 \times 10^6$  reads in serum-derived EVs from AML samples (Fig. 3A and C).

For an overview of mapping distributions, most reads were shown to be unmapped or short. The other reads mainly mapped to rRNAs and miRNAs in both serum H and AML samples. Interestingly, more reads in total and of all types of RNA were detected in AML compared to H samples (Fig. 3A and C).

Since a large proportion of reads were unmapped or shorter than 16 reads, we excluded these reads as well as *no\_adapter* reads and prepared a relative mapping distribution among the

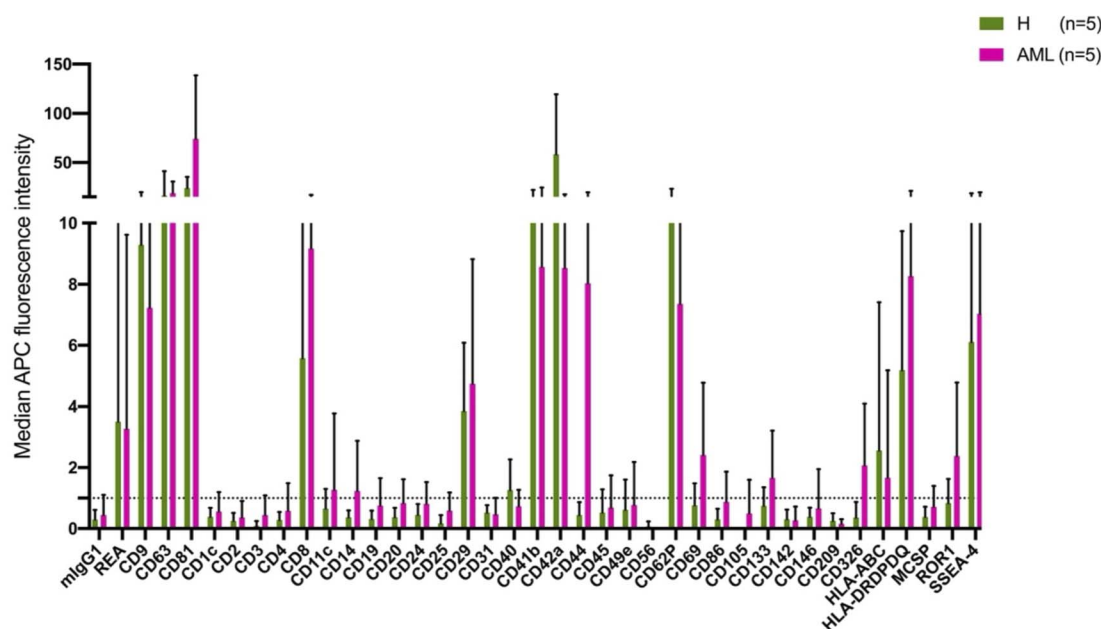
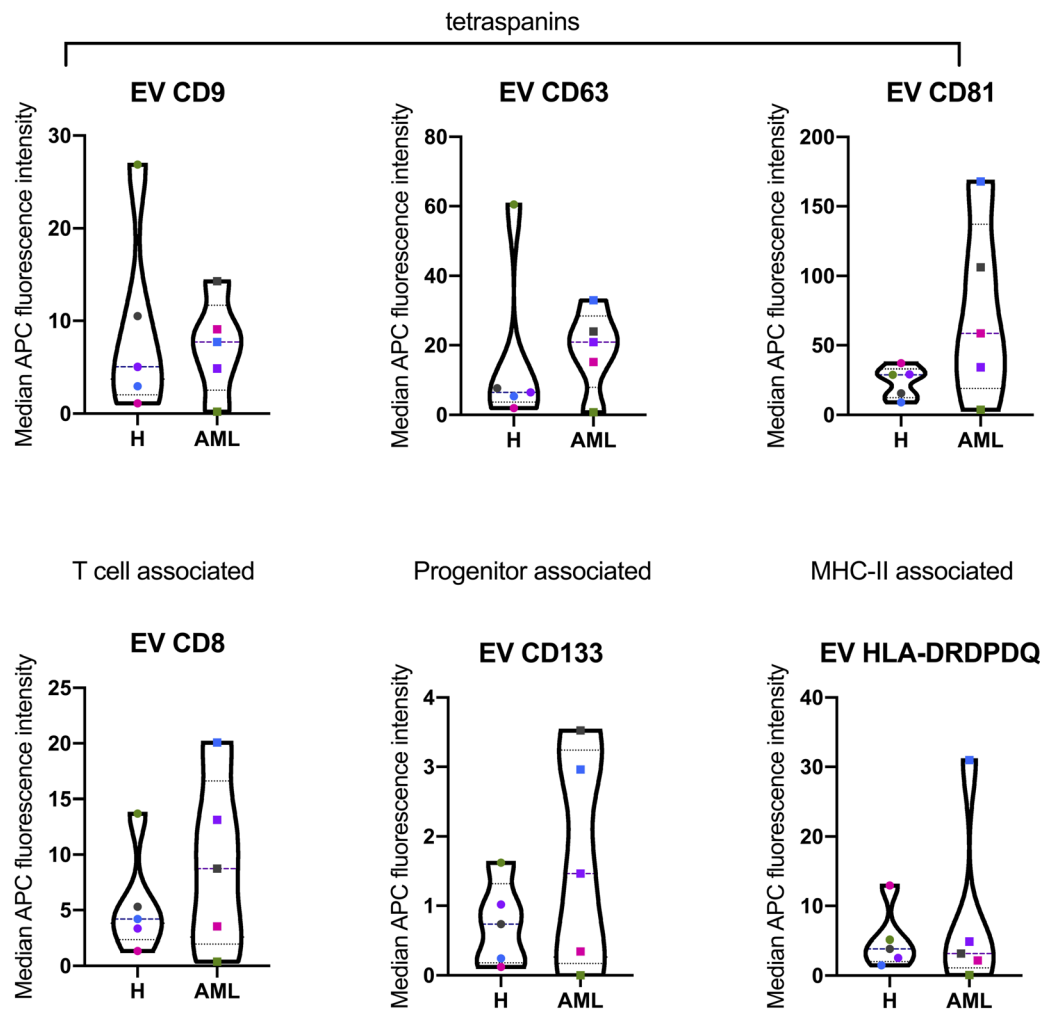


Fig. 1 Characterization of serum derived EVs from H and AML samples by MBFCM. MBFCM allows the detection of EVs (co-) expressing 37 different antigens in a semi-quantitative manner. Results (median APC fluorescence intensities) detected by MBFCM in H (left side, (A)) and AML (right side, (B)) serum samples are displayed. Results are given as mean  $\pm$  SD.





**Fig. 2** Quantification and comparison of EV surface marker expressions from serum derived EVs in H and AML samples with MBFCM. Serum samples were analyzed by multiplex bead-based flow cytometry (MBFCM). Selected several lineage associated EV marker expression on serum from 5 H and 5 AML samples are shown by violin plots (with all individual points) of median APC intensities. Longdash horizontal lines means 'median data', dotted horizontal line means 'quartile data'. For statistical comparison of two groups applying two-way analysis of variance (ANOVA) with Benjamini–Hochberg adjustments were analyzed.

remaining RNA reads. The most abundant category of transcripts was rRNA, followed by miRNA, tRNA, snRNA and snoRNA. Of note, more than 60% of retained reads mapped to rRNA, more than 20% of retained reads mapped to miRNA and smaller fractions to tRNA, snRNA and snoRNA (Fig. 3B and D). Interestingly we found that AML showed a substantially higher proportion of all categories of RNA compared to H (not including miRNA) in relative mapping distributions. Although the absolute miRNA read count was higher in AML samples, the relative mapping distribution of reads mapping to small RNA species showed a higher percentage of miRNAs in H samples.

#### Comparison of miRNA profiles in extracellular vesicles from H vs. AML serum samples

After filtering miRNAs with at least 20 DESeq2-normalized reads 152 miRNAs were retained in H and 159 in AML samples, 136 of which were detected in both H and AML samples (Fig. 4A, ESI table†). 16 miRNAs, (10.5% (16/152) of the detected miRNAs)

were exclusively found in EVs purified from H samples. 23 miRNAs, (14.5% (23/159) of the detected miRNAs) were exclusively found in EVs purified from AML samples (Fig. 4A). Based on the 136 shared miRNAs heatmap analysis depicted different miRNA patterns in H or AML samples (Fig. 4B) emphasized by the high number of miRNAs (45/33.1%) that showed a  $\log_2$  fold change  $>|1|$  (Fig. 4C).

To examine expression differences between H and AML samples in more detail, we selected 5 highly up regulated miRNAs (miR-10a-5p, miR-155-5p, miR-100-5p, miR-146b-5p, let-7a-5p) (Fig. 5A) and 5 highly down regulated miRNAs (miR-185-5p, miR-4433b-3p, miR-199a-5p, miR-451a, miR-151a-3p) identified by small RNA sequencing (Fig. 5B). The largest difference in AML compared to H was detected for miR-10a-5p ( $\log_2\text{FC} = 4.89$ ).

We summarized that EVs could be prepared from healthy and AML serum samples: some EV-derived miRNAs prepared from AML samples are up regulated and others are down



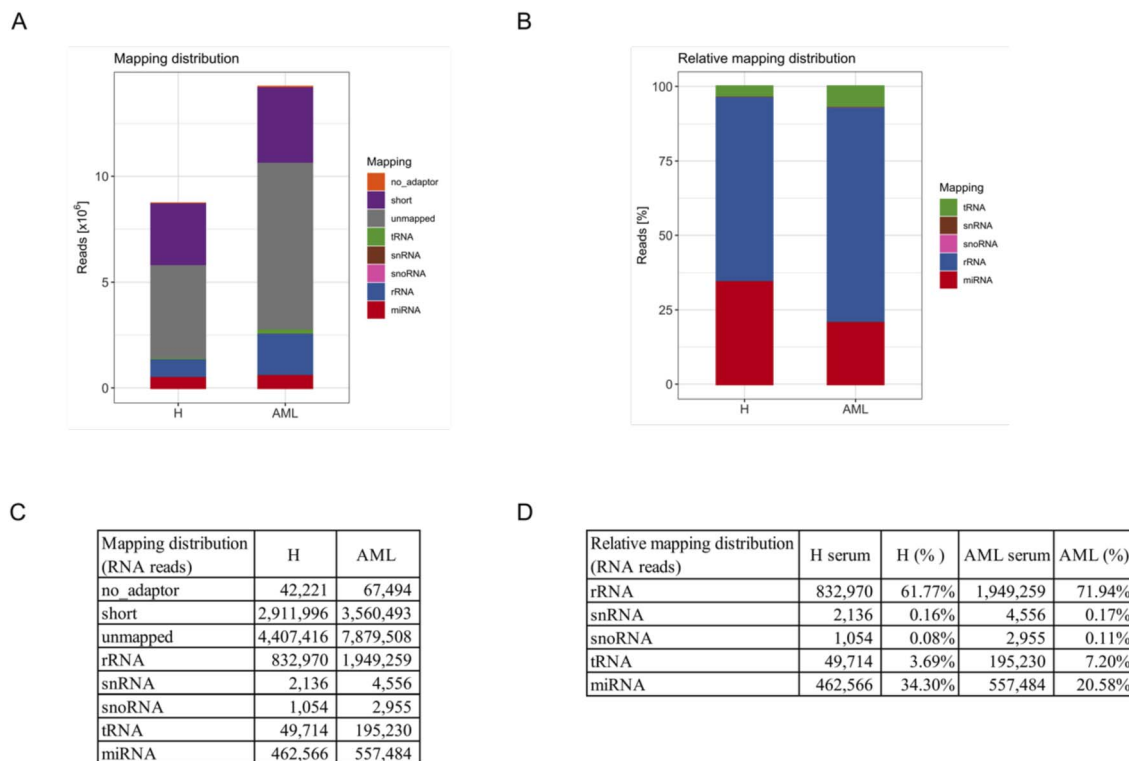


**Fig. 3** Small RNA species in serum derived EVs of H and AML samples. Assignment of small RNA sequencing results to different RNA species from isolated EVs in 5 H and 5 AML serum samples: (A) reads mapping to miRNA, tRNA, snoRNA, snRNA and rRNA, (remained) unmapped, short (shorter than 16 nucleotides) and no-adaptor (no adapter detectable). (B) Relative frequencies of reads that mapped to miRNA, tRNA, snoRNA, snRNA and rRNA (uncharacterized unmapped reads were excluded). (C) Mapping distribution of RNA reads. (D) Relative mapping distribution of RNA reads (uncharacterized unmapped reads were excluded).

regulated compared to healthy samples. These disproportions might indicate physiological changes related to the disease and that these miRNA mechanisms may be affected in AML in different ways.

## Discussion

In this study, we compared serum EV-derived miRNA contents from H and AML patients to assess relevant differences that could qualify as novel non-invasive and RNA-based biomarkers. Both H and AML patient samples were further subjected to MBFCM, which is a reliable method<sup>13,28</sup> to detect and quantify EV surface protein signatures. By applying MBFCM, we demonstrated that serum-derived EVs of H and AML patients both showed high abundancies of the tetraspanins CD9, CD63 and CD81 on their surface (Fig. 1). Several other EV surface markers were detected in blood in accordance with previous findings:<sup>13</sup> T cell EV associated marker CD8, integrin associated EV marker CD29, megakaryocyte (or thrombocyte) associated EV marker CD41b (integrin  $\alpha$ II  $\beta$ ) and CD42a and MHC-II associated EV marker HLA-DRDPDQ could be detected in H as well as AML samples.

Previously it was shown that leukemic blasts can express CD133.<sup>29</sup> Moreover it was shown, that CD133 can be secreted into EVs.<sup>22</sup> Here, we detected elevated levels of CD133 in AML compared to healthy samples by MBFCM, suggesting that

CD133+ EVs were released by AML blasts and subsequently became detectable in human blood. This could mean that these markers (in combination) could qualify as biomarkers to detect even a low tumor load.

In summary, this study presents a proof-of-concept approach to characterize EVs in the blood of AML patients *versus* healthy donors. The authors would like to emphasize that based on the relatively small patient cohort and other limitations (*e.g.* not age matched cohorts) that impact the data no ultimate conclusions can be drawn in terms of specificity for observed differences for AML. Respective differences will have to be confirmed and investigated in larger studies and more complementary upcoming EV analysis methods such as single EV imaging flow cytometry<sup>16</sup> for additional markers and combined subpopulations of EVs, thereby leading to a higher resolution between EV subpopulations. The MBFCM data obtained from this proof-of-concept study still provides some more insight into general expression of EV surface markers in blood of leukemia patients and provides some starting points for future studies.

MiRNA profiles might serve as highly promising biomarkers in AML for improved classification and determination of the appropriate treatment in patients initially presenting with leukemia. Interestingly, specific subtypes and mutant drivers of AML are associated with distinctive miRNA expression profiles, again suggesting that miRNAs could be useful in the initial classification of the disease.<sup>30</sup>



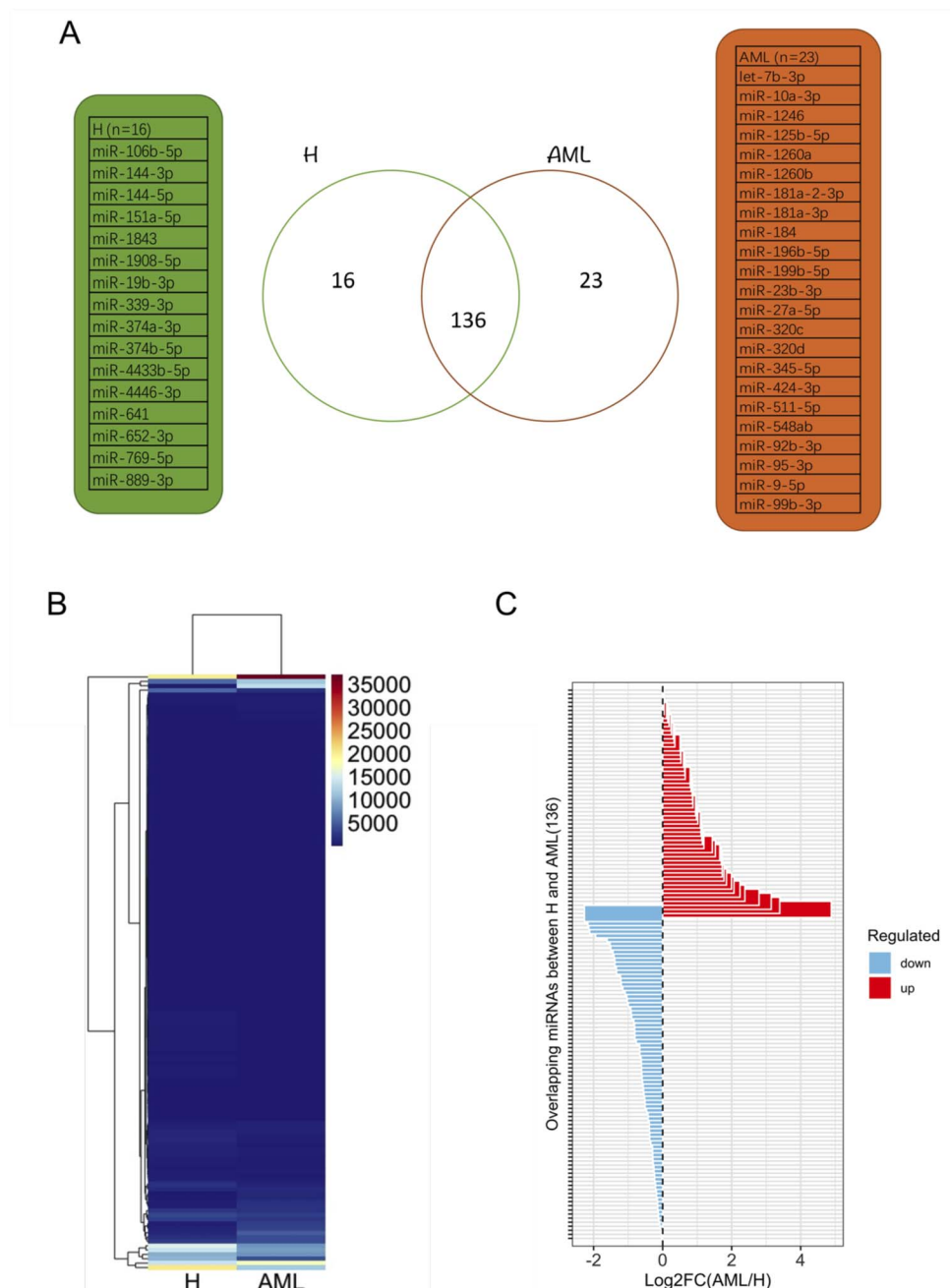


**Fig. 4** Profiling and characterization of DESeq2-normalized miRNA data derived from EVs in H and various expression patterns of miRNAs with more than 20 DESeq2-normalized read counts derived from EVs in H and AML serum samples: (A) Venn diagram of distinct miRNA patterns detected in H and AML samples. (B) Heatmap and hierarchical cluster analysis of H from AML samples. (C) Log<sub>2</sub> fold change (FC) of overlapping miRNAs (136) between H and AML samples.

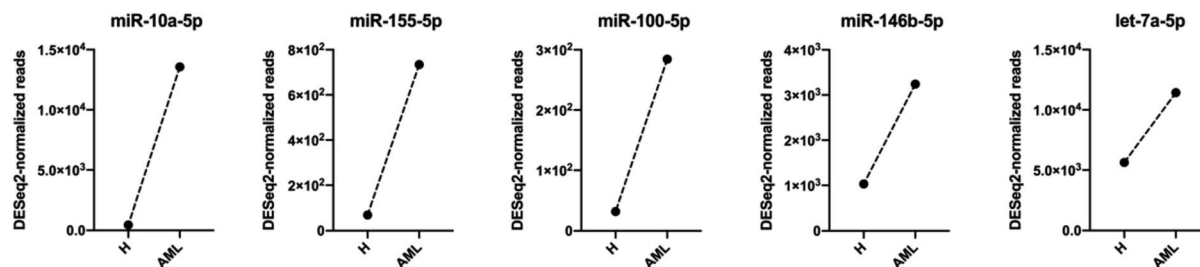
In general miRNAs are known to function as tumor activator or suppressor RNA.<sup>10,19</sup> To obtain a better insight into changes of molecular profiles specific for H in comparison with AML, we focused on the cellular (Table 3) and EV (Table 4) levels of individual miRNAs and observed that ten miRNAs were deregulated in AML patients' samples. In addition to AML, we also identified a large set of other tumors to support or investigate our selected ten miRNAs' function, *e.g.* tumor activator (oncomiR) or suppressor, based on EV level detected by the RNA-Seq.

Concerning cellular derived miRNAs (Table 3), the expression level of miR-10a-5p in AML and myelodysplastic syndrome (MDS) was shown to be significantly higher compared to controls.<sup>7,31</sup> MiR-10a-5p and miR-155-5p are highly expressed in FLT3-ITD associated AMLs.<sup>32</sup> MiR-155 was shown to control B and T-cell differentiation and the development of regulatory T-cells.<sup>17,33,34</sup> Inhibiting miR-155 expression in LPS activated DCs resulted in an increase in pro-inflammatory cytokines gene expression (*e.g.* IL-1 $\alpha$ , IL-1 $\beta$ , IL-6, TNF- $\alpha$  and IL-23).<sup>35</sup> MiR-100





## A Up regulated miRNAs derived from EVs in AML vs. H serum samples



## B Downregulated miRNAs derived from EVs in AML vs. H serum samples

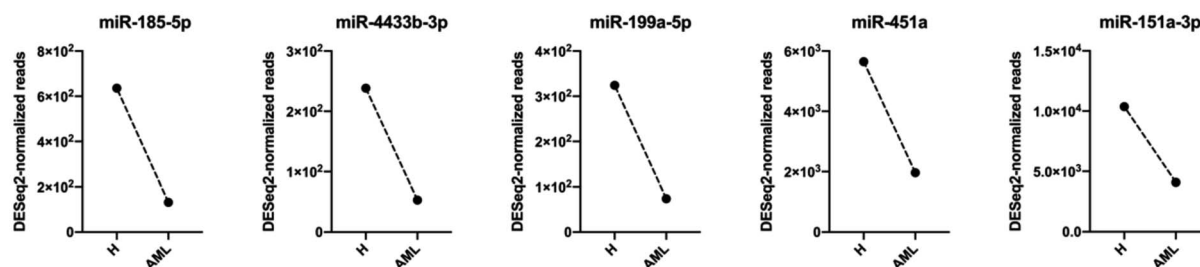


Fig. 5 Selected 10 DESeq2-normalized miRNAs derived from EVs in H and AML serum samples given are up or down regulated miRNAs derived from EVs in AML vs. H serum samples: (A) 5 miRNAs (miR-10a-5p, miR-155-5p, miR-100-5p, miR-146b-5p, let-7a-5p) were up regulated. (B) 5 miRNAs (miR-185-5p, miR-4433b-3p, miR-199a-5p, miR-451a, miR-151a-3p) were down regulated.

expressed highly and regulated cell differentiation and survival by targeting RBSP3 in AML.<sup>36–38</sup> MiR-146b-5p was shown to be significantly increased in MDS patients compared to controls in plasma.<sup>7</sup> In human AML cell lines OCI-AML3, cellular let-7a was shown to be downregulated by SDF-1 $\alpha$ -mediated CXCR4 activation and increased by CXCR4 inhibition.<sup>39</sup> By targeting GPX1, miR-185-5p inhibited AML progression and downregulated AML cells' proliferation and invasion.<sup>40</sup> MiR-185-5p was shown to be associated with the negative regulation of myeloid leukocyte differentiation, negative regulation of myeloid cell differentiation, and positive regulation of hematopoiesis in the regulation of CN-AML.<sup>41</sup> MiR-199a-5p was shown to play an important role in regulating the sensitivity of AML cells to Adriamycin (ADM) treatment.<sup>42</sup>

Concerning EV derived miRNAs (Table 4), miR-10a-5p was significantly increased in MDS, prostate cancer (PCa) and human immunodeficiency virus (HIV) patients compared to controls in plasma derived EVs.<sup>7,43,44</sup> We found miR-155 derived from EVs upregulated in AML, chronic lymphocytic leukemia (CLL) and Waldenström's Macroglobulinemia (WM) compared to controls.<sup>33</sup> Dunand-Sauthier *et al.* found that miR155-induced repression of Arg2 expression appeared critical for DCs to activate T cells by controlling arginine availability in the extracellular environment.<sup>34</sup> EV-associated miR-100-5p was significantly upregulated (>3-fold) in type 1 autoimmune pancreatitis (AIP) patients when compared with controls.<sup>45</sup> MiR-146b-5p was significantly increased in MDS patients compared to controls in EVs.<sup>7</sup> In urinary EVs, miR-146b-5p was exhibited significantly higher expression from patients with muscle-invasive bladder

cancer (MIBC) compared with non-muscle-invasive bladder cancer (NMIBC).<sup>46</sup> Let-7a-5p purified from EVs was upregulated in plasma of both *P. vivax*-infected and *P. falciparum*-infected patients compared to controls.<sup>47</sup> EV derived let-7a-5p was found to be abnormally expressed in brain microvascular pericytes obtained from spontaneous hypertensive rats compared to normotension Wistar Kyoto rats.<sup>48</sup> In addition, let-7a-5p in EVs could also serve as the mechanism contributing to the reduced cell apoptosis and elevated cell autophagy in AKI.<sup>49</sup>

On the other hand, EVs with miR-185-5p as cargo was shown to be elevated in the setting of profound epithelial cell death.<sup>50</sup> Exosomal miRNAs miR-4433b-3p was found downregulated in immune thrombocytopenia (ITP) patients compared to control.<sup>51</sup> EV miR-199a-5p and miR-451a were reduced in higher-risk MDS compared to lower-risk disease.<sup>52</sup> EV miR-199a-5p was associated with three metals (barium, mercury, and thallium) in early pregnancy, and their predicted target genes were enriched in pathways important for placental development.<sup>53</sup> A significant increase of miRNA-451a copies (in EVs) was detected in breast cancer (BC) patients' sera compared to controls.<sup>14</sup> EV miR-451a levels correlated also with the severity of experimental autoimmune encephalomyelitis (EAE).<sup>54</sup> Plasma derived EV miR-151a-3p was shown to be significantly decreased in Alzheimer's disease (AD) compared to controls.<sup>55</sup>

As evidenced in differential gene expression (DGE) analyses based on small RNA-Seq, we focused on 136 shared miRNAs between H and AML (Fig. 4B) and selected ten miRNAs (miR-10a-5p, miR-155-5p, miR-100-5p, miR-146b-5p, let-7a-5p and miR-185-5p, miR-4433b-3p, miR-199a-5p, miR-451a, miR-151a-





Table 3 Selected miRNAs involved in AML pathogenesis<sup>a</sup>

	Cellular sources	Compared to healthy (H)	Confirmed targets	Targeted cells	Functional effect of expression		References
					OncomiR	Tumor suppressor	
miR-10a-5p	Serum, BM, plasma	↑ in AML vs. H (FC = 4.8); ↑ MDS (plasma) vs. H	FLT3-ITD/NPM1, CEBPA, C-KIT, MDM4	nd	↑ cell survival, ↑ cellular growth, and induce angiogenesis, protease inhibitors ↑ chemotherapy drug sensitivity of AML, ↑ pathogenesis of NPM1 mutated (NPM1mut), ↓ MDM4 downregulation	↑ cell survival, ↑ cellular growth, and induce angiogenesis, protease inhibitors ↑ chemotherapy drug sensitivity of AML, ↑ pathogenesis of NPM1 mutated (NPM1mut), ↓ MDM4 downregulation	7, 31 and 32
miR-155- (5p)	BM, plasma, cell lines (KG1 and NB4)	↑ CN-AML vs. H (normal haematopoietic cell)	FLT3-ITD, CEBPB, SHIP1, PU.1	T cells	↑ proliferation, ↑ survival, overexpression leads to myeloproliferative neoplasm in mice, confers negative prognosis in CN-AML, no effect in MLL-AF9 mouse model of leukemia	nd	17 and 32–35
miR-100- (5p)	BM, plasma, cell lines	nd	RBSF3	nd	↑ proliferation, ↑ survival, ↓ differentiation	↓ human granulocyte and monocyte differentiation, ↑ cell survival	36, 37 and 38
miR-146b- 5p	Plasma	↑ MDS (plasma) vs. H	SF3B1, DNMT3A	nd	nd	↓ proliferation, ↓ survival, ↓ NF-kB activation, deletion leads to myeloproliferation	7
let-7a-5p	Cell lines	nd	CXCR4	nd	nd	↓ SDF-1α-mediated CXCR4 activation and ↑ by CXCR4 inhibition, ↓ c-Myc and BCL-XL protein, ↑ chemosensitivity	39
miR-185-5p	Cell lines	nd	GPX1	nd	nd	↓ proliferation, ↓ invasion, ↑ differentiation and apoptosis	40 and 41
miR-443b- 3p	nd	nd	nd	nd	nd	nd	nd
miR-199a- 5p	BM, cell lines (KG1 and NB4)	↓ RR(BM) vs. CR	DRAM1	nd	nd	↑ inducible autophagy, ↑ prosurvival, ↓ drug sensitivity, ↑ chemoresistance upon ADM	42
miR-451a	nd	nd	nd	nd	nd	nd	nd
miR-151a- 3p	Plasma	nd	SF3B1, DNMT3A	nd	nd	nd	7

<sup>a</sup> AML acute myeloid leukemia; H healthy donors; FC fold change; BM: bone marrow; AML-DS down syndrome; PB peripheral blood; MDS myelodysplastic syndromes; LSC: leukemic stem-like cells; RR relapsed/refractory; CR complete remission; ↑ up regulated; ↓ down regulated; nd: no data.

**Table 4** Selected extracellular miRNAs involved in tumor pathogenesis<sup>a</sup>

EV-miRNA	Cellular sources	Compared to healthy (H)	Confirmed targets	Targeted cells	Functional effect of expression		References	Predicted change (serum)
					OncomiR	Tumor suppressor		
miR-10a-5p	MDS, plasma; PCa, cell lines, plasma; HIV, plasma; breast cancer, hepatocellular carcinoma	↑ MDS (plasma derived EV) vs. H; ↑ ( $p = 0.018$ ) PCa (plasma derived EV) vs. H; ↑ (plasma derived EVs) HIV-positive vs. HIV-negative subjects	SF3B1, DNMT3A (MDS)	nd	↓ cell apoptosis ↑ viability of AML cells <i>in vivo</i> and <i>in vitro</i> , oncogene in leukemogenesis	Involved in angiogenesis, transcription actin cytoskeleton, and ephrin receptor signaling	7, 43 and 44	↑
miR-155-5p	HMs (AML, CLL, WM, MDS, MM, FL, DLBCL, HL), serum	↑ AML, CLL, WM (serum derived EV) vs. H	nd	nd	nd	nd	33	↑
miR-100-5p	HucMSC; type 1 AIP, CP, serum	↑ ( $p = 3.23$ ) AIP (serum derived EV) vs. H	NOX4	nd	nd	↓ DOX-induced ROS, LDH, and MDA, ↓ SOD, ↑ apoptotic cells, ↑ NOX4 and cleaved-caspase-3 protein expression	45	↑
miR-146b-5p	MDS, plasma; MIBC, tumor tissues and urinary EV; HIV, plasma	↑ (FC = 7.84; $P = 0.004$ ) (urinary EVs) MIBC vs. NMIBC patients; ↑ (plasma derived EVs) HIV-positive vs. HIV-negative	SF3B1, DNMT3A (MDS)	nd	↓ cell apoptosis ↑ viability of AML cells <i>in vivo</i> and <i>in vitro</i> , oncogene in leukemogenesis	nd	7, 44 and 46	↑
let-7a-5p	Brain microvascular pericytes from SHR; plasma of Thai <i>P. vivax</i> -infected patients	Abnormally expressed in brain microvascular pericyte EVs of SHR vs. WKY rats	TGF-β pathway	nd	nd	Brain microvascular pericytes and the pathogenesis of hypertension	47 and 48	↑
miR-185-5p	Murine model (mimics human ARDS), cell lines	↑ hyperoxia vs. Room air, ↑ mimics vs. control	FADD/caspase-8	nd	nd	↓ FADD and caspase-8, ↑ necroptosis	50	↓
miR-4433b-3p	ITP, plasma	↓ ITP (plasma derived EV) vs. H	nd	nd	nd	nd	51	↓
miR-199a-5p	MDS, plasma; pregnancy	↓ MDS (plasma derived EV) ( $p < 0.05$ ) vs. H	nd	nd	nd	nd	7, 52 and 53	↓
miR-451a	MDS, plasma; BC, AD, DLB, murine EAE	↓ MDS (plasma derived EV) ( $p < 0.05$ ) vs. H; ↑ BC (serum derived EV) vs. H; ↓ AD (plasma derived EV) vs. H	AKT1, CAB39 (BC)	nd	nd	Involved in neuron differentiation-proliferation and death, genes related to SMAD protein phosphorylation, affects the central nervous system	14, 52 and 54	↓



Table 4 (Contd.)

EV-miRNA	Cellular sources	Compared to healthy (H)	Confirmed targets	Targeted cells	Functional effect of expression		Predicted change (serum)
					OncomiR	Tumor suppressor	
miR-151-3p	MDS plasma; AD, plasma	↓ AD (plasma derived EV) v.s. H	SF3B1, DNMT3A (MDS)	nd	↓ cell apoptosis ↑ viability of AML cells <i>in vivo</i> and <i>in vitro</i> , oncogene in leukemogenesis	nd	↓

<sup>a</sup> AML acute myeloid leukemia; CLL chronic lymphocytic leukemia; WM Waldenstrom's macroglobulinemia; MDS myelodysplastic syndrome; MM multiple myeloma, FL follicular lymphoma, DLBCL diffuse large B-cell lymphoma; HL Hodgkin's lymphoma; H healthy donors; HuCMSC human umbilical cord mesenchymal stem cells; AIP autoimmune pancreatitis; CP chronic pancreatitis; FC fold change; BM bone marrow; MIBC muscle-invasive bladder cancer; SHR spontaneous hypertensive rats; PCa prostate cancer; HIV human immunodeficiency virus; ARDS acute respiratory distress syndrome; ITP Immune thrombocytopenia; AD Alzheimer's disease; DLB dementia with Lewy bodies; BC breast cancer; EAE experimental autoimmune encephalomyelitis; ↑ up regulated; ↓ down regulated; nd no data.

3p) expressed with  $\log_2FC > |1|$  (Fig. 4C). The highest fold change ( $\log_2FC = 4.89$ ) was detected for EV-derived miR-10a-5p, which was upregulated in AML compared to H. It is well known that, miRNAs impact disease development and progression through collaboration with known oncogenes or tumor suppressors, either by directly targeting them on the mRNA level or by working in concert with resulting proteins to promote malignancy.

In this study, we found miR-10a-5p derived from EVs ( $\log_2FC = 4.89$ ) upregulated in AML compared to H samples, which might confirm a direct correlation between EV miR-10a-5p level with poor prognosis in leukemic patients.<sup>31</sup> miR-155-5p derived from EVs was also upregulated ( $\log_2FC = 3.39$ ) in AML compared to H samples, which might suggest that EV-associated miR-155 deficiency in these hematologic compartments may cause attenuated immune regulation. Our findings confirm that miR-100-5p, miR-146b-5p and let-7a-5p derived from EVs were upregulated in AML compared to H samples. Let-7a-5p might regulate genes involved in adherents junction or transforming growth factor- $\beta$  pathways.

Interestingly, our data showed that miR-185-5p ( $\log_2FC = -2.27$ ) from serum derived EVs was down regulated in AML compared to H samples, what might support that miR-185-5p in extracellular vesicles might be a key regulator of pathological processes. Our serum data also showed that miR-4433b-3p, miR-199a-5p, miR-451a and miR-151a-3p derived from EVs were down regulated in AML compared to H samples. These EV derived miRNAs have been shown to accumulate phosphorylation enzymes, proteasome-related proteins and genes involved in cell death among others and could therefore point to sufficiently altered metabolic processes.

## Conclusions

In summary, we demonstrate that MBFCM is generally suitable for EV characterization in minimally processed AML samples. Our data indicates that EV-derived miRNA cargo changes between H and AML might not only reflect differences in levels of many hematopoiesis-related, but also general metabolic differences. In particular, miRNAs derived from EVs could be considered privileged players as biomarkers due to their impact on target cells and tissues, and we assume that EV derived miRNA dysregulation in blood circulation by tumor activators (oncomiR) or tumor suppressors could have a significant impact on multiple recipient cells, affecting their physiological features and contributing to the development of myelodysplasia.

## Abbreviations

AML	Acute myeloid leukemia
H	Healthy
MDS	Myelodysplastic syndrome
EV(s)	Extracellular vesicle(s)
WB	Whole blood
TEM	Transmission electron microscopy



fNTA	Fluorescence nanoparticle tracking analysis
RNA-Seq	RNA sequencing
miRNA	MicroRNA
mRNA	Messenger RNA
rRNA	Ribosomal RNA
snRNA	Small nuclear RNA
snoRNA	Small nucleolar RNA
tRNA	Transfer RNA
nm	Nanometer(s)
nt	Nucleotide(s)
RIN	RNA integrity number
AML-DS	Acute myeloid leukemia-down syndrome
PB	Peripheral blood
LSC	Leukemic stem-like cells
RR	Relapsed/refractory
CR	Complete remission
WM	Waldenström's macroglobulinemia
MM	Multiple myeloma
FL	Follicular lymphoma
DLBCL	Diffuse large B-cell lymphoma
HL	Hodgkin's lymphoma
HucMSC	Human umbilical cord mesenchymal stem cells
AIP	Autoimmune pancreatitis
CP	Chronic pancreatitis
FC	Fold change
BM	Bone marrow
SHR	Spontaneous hypertensive rats
MIBC	Muscle-invasive bladder cancer
NMIBC	Non-muscle-invasive bladder cancer
PCa	Prostate cancer
HIV	Human immunodeficiency virus
ARDS	Acute respiratory distress syndrome
ITP	Immune thrombocytopenia
AD	Alzheimer's disease
DLB	Dementia with Lewy bodies
BC	Breast cancer
EAE	Experimental autoimmune encephalomyelitis

## Availability of data and material

All human blood samples and medical reports were provided from the University Hospitals of Munich, Stuttgart and Augsburg.

## Ethics statement

All blood sampling was conducted after obtaining patients' written informed consent in accordance with the World Medical Association Declaration of Helsinki and the ethic committee of the Ludwig-Maximilians-University-Hospital Munich, Pettenkoferstr. 8a, 80336 Munich, Ludwig-Maximilians-University Hospital in Munich; Vote-no. 339-05.

## Data availability

All data generated or analysed during this study are included in this published article [and are given as ESI† files] or are available from the corresponding authors on request.

## Author contributions

H. M. S., L. L., V. M. and M. W. P. designed the study. H. M. S., L. L. and V. M. contributed to the writing, review and discussion of the manuscript. L. L., E. P., A. S. H., H. A., E. R., prepared serum supernatants and conducted cell-culture experiments and clinical reports and statistical-analysis. A. R. and J. S. provided leukemic samples and corresponding patients' diagnostic reports. A. G. conducted MBFCA experiments, provided discussion of the project and revised the manuscript. V. M. conducted miRNA sequencing experiments and provided statistical analyses and graphical illustration thereof. V. M. and M. W. P. took part in the discussion of the results and revised the manuscript.

## Conflicts of interest

All authors declare that there are no financial conflicts in regard to this work.

## Acknowledgements

The project was supported by intramural funding of M. P. A. G. has got a scholarship of the International Society for Advancement of Cytometry (ISAC) Marylou Ingram Scholars program 2019–2023. L. L. was funded by grants of China Scholarship Council (CSC) (File No. 201808210307). The funders had no role in the study design, data collection and analysis, decision to publish, or preparation of the manuscript. The authors thank patients, nurses, and physicians on the wards for their support and the diagnostic laboratories as well as the treating institutions for the patients' diagnostic reports. The results presented in this manuscript were worked out in the PhD thesis of Lin Li at the University Hospital of the Ludwig-Maximilian-University Munich.

## References

- 1 H. Döhner, E. Estey, D. Grimwade, *et al.*, Diagnosis and management of AML in adults: 2017 ELN recommendations from an international expert panel, *Blood*, 2017, **129**(4), 424–447.
- 2 D. Cancilla, M. P. Rettig and J. F. DiPersio, Targeting CXCR4 in AML and ALL, *Front. Oncol.*, 2020, **10**, 1672.
- 3 C. L. Boeck, D. C. Amberger, F. Dorane-Gard, *et al.*, Significance of Frequencies, Compositions, and/or Antileukemic Activity of (DC-stimulated) Invariant NKT, NK and CIK Cells on the Outcome of Patients with AML, ALL and CLL, *J. Immunother.*, 2017, **40**(6), 224–248.
- 4 D. Moussa Agha, R. Rouas, M. Najjar, *et al.*, Impact of Bone Marrow miR-21 Expression on Acute Myeloid Leukemia T Lymphocyte Fragility and Dysfunction, *Cells*, 2020, **9**(9), 1–18.
- 5 C. Théry, K. W. Witwer, E. Aikawa, *et al.*, Minimal information for studies of extracellular vesicles 2018 (MISEV2018): a position statement of the International Society for Extracellular Vesicles and update of the





- MISEV2014 guidelines, *J. Extracell. Vesicles*, 2018, 7(1), 1535750.
- 6 M. Boyiadzis and T. L. Whiteside, The emerging roles of tumor-derived exosomes in hematological malignancies, *Leukemia*, 2017, 31(6), 1259–1268.
  - 7 A. Hrustincova, Z. Krejcik, D. Kundrat, *et al.*, Circulating Small Noncoding RNAs Have Specific Expression Patterns in Plasma and Extracellular Vesicles in Myelodysplastic Syndromes and Are Predictive of Patient Outcome, *Cells*, 2020, 9(4), 794.
  - 8 S. Huang, Y. Li, P. Wu, *et al.*, microRNA-148a-3p in extracellular vesicles derived from bone marrow mesenchymal stem cells suppresses SMURF1 to prevent osteonecrosis of femoral head, *J. Cell. Mol. Med.*, 2020, 24(19), 11512–11523.
  - 9 S. Hao, O. Bai, J. Yuan, M. Qureshi and J. Xiang, Dendritic cell-derived exosomes stimulate stronger CD8<sup>+</sup> CTL responses and antitumor immunity than tumor cell-derived exosomes, *Cell. Mol. Immunol.*, 2006, 3(3), 205–211.
  - 10 V. Mussack, G. Wittmann and M. W. Pfaffl, Comparing small urinary extracellular vesicle purification methods with a view to RNA sequencing—Enabling robust and non-invasive biomarker research, *Biomol. Detect. Quantif.*, 2019, 17, 100089.
  - 11 D. Buschmann, B. Kirchner, S. Hermann, *et al.*, Evaluation of serum extracellular vesicle isolation methods for profiling miRNAs by next-generation sequencing, *J. Extracell. Vesicles*, 2018, 7(1), 1481321.
  - 12 D. Buschmann, V. Mussack and J. B. Byrd, Separation, characterization, and standardization of extracellular vesicles for drug delivery applications, *Adv. Drug Delivery Rev.*, 2021, 174, 348–368.
  - 13 O. P. B. Wiklander, R. B. Bostancioglu, J. A. Welsh, *et al.*, Systematic methodological evaluation of a multiplex bead-based flow cytometry assay for detection of extracellular vesicle surface signatures, *Front. Immunol.*, 2018, 9, 1326.
  - 14 B. M. Moloney, K. E. Gilligan, D. P. Joyce, *et al.*, Investigating the Potential and Pitfalls of EV-Encapsulated MicroRNAs as Circulating Biomarkers of Breast Cancer, *Cells*, 2020, 9(1), 1–13.
  - 15 N. I. Hornick, J. Huan, B. Doron, *et al.*, Serum Exosome MicroRNA as a minimally-invasive early biomarker of AML, *Sci. Rep.*, 2015, 5, 11295.
  - 16 A. Görgens, M. Bremer, R. Ferrer-Tur, *et al.*, Optimisation of imaging flow cytometry for the analysis of single extracellular vesicles by using fluorescence-tagged vesicles as biological reference material, *J. Extracell. Vesicles*, 2019, 8(1), 1587567.
  - 17 J. A. Wallace and R. M. O'Connell, MicroRNAs and acute myeloid leukemia: Therapeutic implications and emerging concepts, *Blood*, 2017, 130(11), 1290–1301.
  - 18 Q. Guo, J. Luan, N. Li, *et al.*, MicroRNA-181 as a prognostic biomarker for survival in acute myeloid leukemia: A meta-analysis, *Oncotarget*, 2017, 8(51), 89130–89141.
  - 19 H. Tadokoro, T. Umezū, K. Ohyashiki, T. Hirano and J. H. Ohyashiki, Exosomes derived from hypoxic leukemia cells enhance tube formation in endothelial cells, *J. Biol. Chem.*, 2013, 288(48), 34343–34351.
  - 20 B. Mateescu, E. J. K. Kowal, B. W. M. van Balkom, *et al.*, Obstacles and opportunities in the functional analysis of extracellular vesicle RNA - An ISEV position paper, *J. Extracell. Vesicles*, 2017, 6(1), 1286095.
  - 21 D. C. Amberger, F. Dorane-Gard, C. Gunsilius, *et al.*, PGE1-containing protocols generate mature (leukemia-derived) dendritic cells directly from leukemic whole blood, *Int. J. Mol. Sci.*, 2019, 20(18), 4590.
  - 22 L. Li, V. Mussack and E. Pepeldjyska, *et al.*, Description and optimization of a multiplex bead-based flow cytometry method (MBFCM) to characterize extracellular vesicles in serum samples from patients with hematological malignancies, 2022, 29(11), pp. 1600–1615.
  - 23 S. Andrews, *FastQC - A Quality Control Tool for High Throughput Sequence Data*, Babraham Bioinformatics, 2010, <https://www.bioinformatics.babraham.ac.uk/projects/fastqc/>.
  - 24 Y. Kong, Btrim: A fast, lightweight adapter and quality trimming program for next-generation sequencing technologies, *Genomics*, 2011, 98(2), 152–153.
  - 25 The RNA Central Consortium, RNAcentral: a hub of information for non-coding RNA sequences The RNAcentral Consortium 1–38, *Nucleic Acids Res.*, 2018, 47(D1), D221–D229.
  - 26 A. Kozomara and S. Griffiths-Jones, MiRBase: Annotating high confidence microRNAs using deep sequencing data, *Nucleic Acids Res.*, 2014, 42(D1), D68–D73.
  - 27 B. Langmead, C. Trapnell, M. Pop and S. L. Salzberg, Ultrafast and memory-efficient alignment of short DNA sequences to the human genome, *Genome Biol.*, 2009, 10(3), R25.
  - 28 N. Koliha, Y. Wiencek, U. Heider, *et al.*, A novel multiplex bead-based platform highlights the diversity of extracellular vesicles, *J. Extracell. Vesicles*, 2016, 5(1), 29975.
  - 29 F. M. Tolba, M. E. Foda, H. M. Kamal and D. A. Elshabrawy, Expression of CD133 in acute leukemia, *Med. Oncol.*, 2013, 30(2), 527.
  - 30 S. Mi, J. Lu, M. Sun, *et al.*, MicroRNA expression signatures accurately discriminate acute lymphoblastic leukemia from acute myeloid leukemia, *Proc. Natl. Acad. Sci. U. S. A.*, 2007, 104(50), 19971–19976.
  - 31 Y. Zhi, X. Xie, R. Wang, *et al.*, Serum level of miR-10-5p as a prognostic biomarker for acute myeloid leukemia, *Int. J. Hematol.*, 2015, 102(3), 296–303.
  - 32 D. Gerloff, A. A. Wurm, J.-U. Hartmann, *et al.*, Next Generation Sequencing and Functional Analysis of Mirna Expression in Acute Myeloid Leukemia Patients with Different FLT3 Mutations: Block of MiR-155 in FLT3-ITD Driven AML Leads to Downregulation of Myeloid Blasts in Vivo, *Blood*, 2015, 126(23), 2438.
  - 33 A. Caivano, F. La Rocca, V. Simeon, *et al.*, MicroRNA-155 in serum-derived extracellular vesicles as a potential biomarker for hematologic malignancies - a short report, *Cell. Oncol.*, 2017, 40(1), 97–103.



- 34 I. Dunand-Sauthier, M. Irla, S. Carnesecchi, *et al.*, Repression of Arginase-2 Expression in Dendritic Cells by MicroRNA-155 Is Critical for Promoting T Cell Proliferation, *J. Immunol.*, 2014, **193**(4), 1690–1700.
- 35 L. A. Smyth, D. A. Boardman, S. L. Tung, R. Lechler and G. Lombardi, MicroRNAs affect dendritic cell function and phenotype, *Immunology*, 2015, **144**(2), 197–205.
- 36 Y. S. Zheng, H. Zhang, X. J. Zhang, *et al.*, MiR-100 regulates cell differentiation and survival by targeting RBSP3, a phosphatase-like tumor suppressor in acute myeloid leukemia, *Oncogene*, 2012, **31**(1), 80–92.
- 37 Z. Krejcik, M. Belickova, A. Hrustincova, *et al.*, MicroRNA profiles as predictive markers of response to azacitidine therapy in myelodysplastic syndromes and acute myeloid leukemia, *Cancer Biomarkers*, 2018, **22**(1), 101–110.
- 38 L. Garcia-Orti, I. Cristobal and M. Marcotegui, *et al.*, Integration of global snp-based mapping and expression arrays with microrna patterns reveals deregulated mirnas and their gene candidate targets in acute myeloidleukemia, *Haematologica*, 2010, 95.
- 39 Y. Chen, R. Jacamo, M. Konopleva, *et al.*, CXCR4 downregulation of let-7a drives chemoresistance in acute myeloid leukemia, *J. Clin. Invest.*, 2013, **123**(6), 2395–2407.
- 40 B. Pang, H. Mao, J. Wang and W. Yang, MiR-185-5p suppresses acute myeloid leukemia by inhibiting GPX1, *Microvasc. Res.*, 2022, **140**, 104296.
- 41 E. Esa, A. K. Hashim, E. H. M. Mohamed, *et al.*, Construction of a microRNA-mRNA Regulatory Network in de Novo Cytogenetically Normal Acute Myeloid Leukemia Patients, *Genet. Test. Mol. Biomarkers*, 2021, **25**(3), 199–210.
- 42 Y. Li, G. Zhang, B. Wu, W. Yang and Z. Liu, MiR-199a-5p Represses Protective Autophagy and Overcomes Chemoresistance by Directly Targeting DRAM1 in Acute Myeloid Leukemia, *J. Oncol.*, 2019, **2019**, 5613417.
- 43 T. S. Worst, C. Previti, K. Nitschke, *et al.*, Mir-10a-5p and mir-29b-3p as extracellular vesicle-associated prostate cancer detection markers, *Cancers*, 2020, **12**(1), 43.
- 44 S. Chettimada, D. R. Lorenz, V. Misra, S. M. Wolinsky and D. Gabuzda, Small RNA sequencing of extracellular vesicles identifies circulating miRNAs related to inflammation and oxidative stress in HIV patients, *BMC Immunol.*, 2020, **21**(1), 1–20.
- 45 K. Nakamaru, T. Tomiyama, S. Kobayashi, *et al.*, Extracellular vesicles microRNA analysis in type 1 autoimmune pancreatitis: Increased expression of microRNA-21: miR-21 and type 1 AIP, *Pancreatology*, 2020, **20**(3), 318–324.
- 46 S. Baumgart, P. Meschkat, P. Edelmann, *et al.*, MicroRNAs in tumor samples and urinary extracellular vesicles as a putative diagnostic tool for muscle-invasive bladder cancer, *J. Cancer Res. Clin. Oncol.*, 2019, **145**(11), 2725–2736.
- 47 N. Ketprasit, I. S. Cheng, F. Deutsch, *et al.*, The characterization of extracellular vesicles-derived microRNAs in Thai malaria patients, *Malar. J.*, 2020, **19**(1), 1–14.
- 48 Q. Wu, X. Yuan, B. Li, *et al.*, Differential miRNA expression analysis of extracellular vesicles from brain microvascular pericytes in spontaneous hypertensive rats, *Biotechnol. Lett.*, 2020, **42**(3), 389–401.
- 49 C. Zhang, Y. Shang, X. Chen, *et al.*, Supramolecular Nanofibers Containing Arginine-Glycine-Aspartate (RGD) Peptides Boost Therapeutic Efficacy of Extracellular Vesicles in Kidney Repair, *ACS Nano*, 2020, **14**(9), 12133–12147.
- 50 J. M. Carnino, H. Lee, X. He, M. Groot and Y. Jin, Extracellular vesicle-cargo miR-185-5p reflects type II alveolar cell death after oxidative stress, *Cell Death Discovery*, 2020, **6**(1), 82.
- 51 Y. Sun, Y. Hou, G. Meng, *et al.*, Proteomic analysis and microRNA expression profiling of plasma-derived exosomes in primary immune thrombocytopenia, *Br. J. Haematol.*, 2021, **194**(6), 1045–1052.
- 52 M. Dostalova Merkerova, A. Hrustincova, Z. Krejcik, *et al.*, Microarray profiling defines circulating microRNAs associated with myelodysplastic syndromes, *Neoplasma*, 2017, **64**(4), 571–578.
- 53 C. G. Howe, H. B. Foley, S. F. Farzan, *et al.*, Urinary metals and maternal circulating extracellular vesicle microRNA in the MADRES pregnancy cohort, *Epigenetics*, 2021, **17**(10), 1128–1142.
- 54 M. Nakashima, K. Ishikawa, A. Fugiwara, *et al.*, miR-451a levels rather than human papillomavirus vaccine administration is associated with the severity of murine experimental autoimmune encephalomyelitis, *Sci. Rep.*, 2021, **11**(1), 1–13.
- 55 A. Gámez-Valero, J. Campdelacreu, D. Vilas, *et al.*, Exploratory study on microRNA profiles from plasma-derived extracellular vesicles in Alzheimer's disease and dementia with Lewy bodies, *Transl. Neurodegener.*, 2019, **8**(1), 1–17.

